Supporting Information

Colocalization of Light Harvesting and Catalytic Units in 'Soft' Coordination Polymer Hydrogel toward Visible-Light Driven Photocatalytic Hydrogen Production

Parul Verma, Ashish Singh, Faruk Ahamed Rahimi, Tapas Kumar Maji*

*Molecular Materials Laboratory, School of Advanced Materials (SAMat), Chemistry and Physics of Materials Unit, Jawaharlal Nehru Centre for Advanced Scientific Research, Bangalore- 560064, India.

*Email: tmaji@jncasr.ac.in

S1. Materials and Methods

9,10-dibromoanthracene, methyl-4-carboxyphenyl boronic acid, 1,3-diaminopropane, 4′-chloro-2,2′:6′,2″-terpyridine, Thionyl chloride ($SOCl_2$), Cesium Fluoride (CsF), Tetrakis-(triphenylphosphine)palladium(0) ($Pd(PPh_3)_4$), Zinc chloride ($ZnCl_2.6H_2O$) were purchased from Sigma-Aldrich chemical Co. Ltd. Solvents were pre-dried using standard procedures. Spectroscopic grade solvents were used for all spectroscopic studies without further purification. UV-Vis absorption studies were carried on a Perkin-Elmer lambda 900 spectrophotometer. Fluorescence studies were accomplished using Perkin Elmer Ls 55 Luminescence spectrometer. ^{1}H-NMR spectra were recorded on a Bruker AVANCE-400 spectrometer (at 600 MHz) with chemical shifts recorded as ppm, and all spectra were calibrated against TMS. ^{13}C-spectrum was recorded at 150 MHz frequency using a Varian Inova 600 MHz spectrometer. UV-Vis spectra were recorded in a Perkin-Elmer lambda 900 spectrometer. The IR experiment measurements were carried out using FT-IR spectrophotometer (BRUKER, VORTEX 70B) in the region 4000−400 cm^{-1}. Thermal stability of materials (xerogel state) was studied using Mettler Toledo TGA 850 instrument in the temperature range of 30-800°C with the heating rate of 5°C/min in N_2 atmosphere. Elemental analyses were carried out using a Thermo Scientific Flash 2000 CHN analyzer. MALDI has performed on a Bruker daltonics Autoflex Speed MALDI TOF System (GT0263G201) spectrometer. High-resolution mass spectrometry was carried out using Agilent Technologies 6538 UHD Accurate-Mass Q-TOFLC/MS. The pH measurements of photocatalytic solvent medium were carried out by Orion Star A211 pH meter. The rheological study was done in Anton Paar Rheometer MCR 302. The PXRD patterns were measured by a Bruker D8 Discover instrument using Cu Kα radiation.

Sample preparation for different studies:

Preparation of Dry Gel samples (Xerogels): For preparation of xerogels, Tousimis Autosamdri@931 was used for critical-point drying (CPD) to preserve the structure of the hydrogel samples. After gel preparation, the water was exchanged with ethanol using a gradient of ethanol/water mixtures (40% to 100 %). Next, the ethanol exchanged gel samples were then transferred to a stainless-steel cage with wire mesh followed by critically point dried with supercritical CO_2.

Transmission electron microscopy: Transmission Electron Microscopy (TEM) studies were done on JEOL JEM -3010 with an accelerating voltage of 300 kV. For analysis of the xerogels, the samples were dispersed in ethanol and drop casted on a lacey carbon film supported on a TEM copper grid. The morphology of self-assembly in hydrogel state of catalyst was observed by coating 5.0 μL droplet of gelator solution on a lacey carbon film supported on a TEM copper grid. After drying the grid under vacuum, the morphology of sample was observed.

Field Emission-Scanning electron microscopy (FE-SEM): The FE-SEM images and Energy-dispersive X-ray spectroscopy (EDAX) analysis were recorded on a Nova Nanosem 600 FEI instrument. The xerogels were dispersed in ethanol and then drop-casted onto a small piece of silicon wafer followed by gold (Au) sputtering for FE-SEM measurements.

Rheology: Rheological measurements were performed by operating in a 25 mm cone-and-plate configuration with a 0.5° cone angle. The rheology experiment was performed using the amplitude sweep method over strain range from 0.01 % to 100 % for hydrogel. For each measurements 25 mg of sample was loaded onto the rheometer plate.

Powder X-ray diffraction (PXRD): The gel sample was coated on a quartz plate uniformly by spin coater and the PXRD pattern was collected in the gel state.

Time-resolved photoluminescence (TRPL): The TRPL studies were performed in Edinburgh instrument (FLS 1000). The decay spectra were recorded using 370 nm laser for excitation. Gel samples were coated on quartz plate and dried under vacuum before the measurements.

Electron paramagnetic resonance (EPR): The EPR studies were performed on JES-X320 (using X-band microwave ES-11030MWU; JEOL Resonance). The EPR data were collected for xerogel of samples to avoid the water interference. The EPR spectra of the samples were monitored after irradiation under visible light for 10 minutes (Schott KL 1600 LED light (1418057: λ>400 nm).

S2. Synthesis of Low Molecular Weight Gelator (LMWG) based linker (TPY-ANT):

Synthesis of TPY-ANT is described in the following steps:

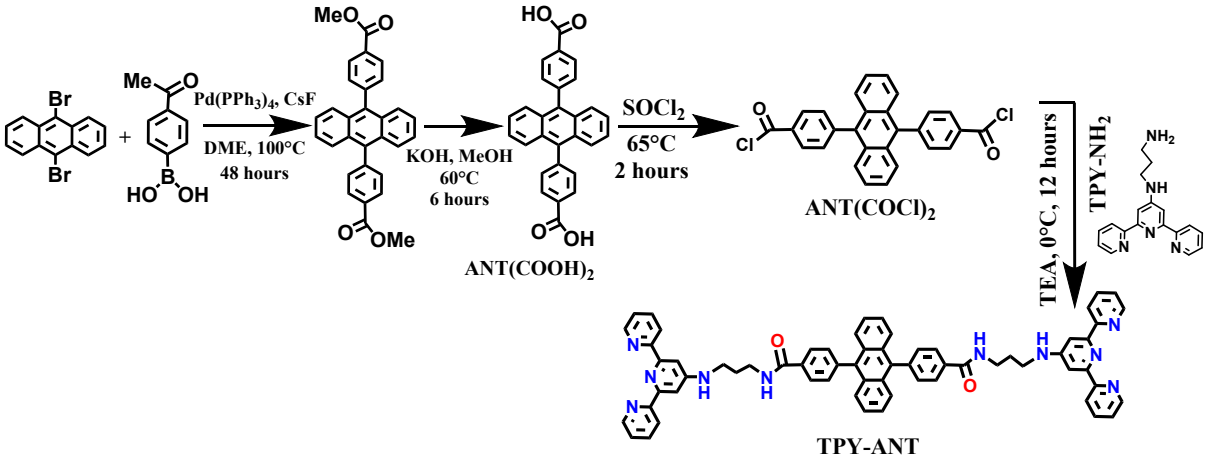

Scheme S1: Synthetic scheme for **TPY-ANT** LMWG.

Step 1. Synthesis of 9,10-(4-carboxyphenyl)anthracene [(ANT(COOH)$_2$]: Synthesis of ANT(COOH)$_2$ is reported earlier by our group.[1] We have followed here the similar procedure and characterization data was in good agreement with the earlier report. 9,10-dibromoanthracene (740 mg, 2.2 mmol), methyl-4-carboxyphenyl boronic acid (1 g, 5.5 mmol), CsF (4 g, 2.7 mmol) and $Pd(PPh_3)_4$ (200 mg, 0.17 mmol)) were suspended in 1,2-dimethoxyethane (30 ml). The reaction mixture was refluxed at 100 ºC for 48 hours under inert condition. After that, the reaction mixture was cooled to room temperature and 100 ml H_2O was added to dissolve the excess CsF, and the organic product was extracted by $CHCl_3$. Crude (ANT(COOH)$_2$ was purified through the column chromatography using chloroform/hexane as eluent. Yield: 93%. The as-prepared (ANT(COOH)$_2$ (563 mg, 1.26 mmol) was suspended in MeOH (30 ml). KOH (425 mg, 7.56 mmol)) was added and refluxed for 6 hours at 60 ºC. After cooling to room temperature, 6N HCl was added drop-wise into the reaction mixture. The white precipitate was formed which was washed repeatedly by cold water and dried under vacuum. Yield: 94 %. ^{1}H-NMR (400 MHz, $CDCl_3$) δ: 8.23 (d, 4H, ArH), 7.62 (m, 4H, ArH), 7.55 (m, 4H, ArH), 7.46 (m, 4H, ArH), 13.11 (2H, COOH). Selected FTIR data (KBr, cm^{-1}): 2986 (b), 2667 (m), 2547 (m), 1688 (s, sh), 1608 (s), 1425 (m), 1291 (m), 769 (m). CHN analysis for $C_{28}H_{18}O_4$: Calc. C, 80.38; H, 4.30%. Expt.: C, 80.41; H, 4.16%.

Step 2. Synthesis of 2,2′:6′,2″-terpyridin-4´-yl-propane-1,3-diamine (TPY-NH_2):

The 2′;6′,2″-terpyridin-4′-yl-propane-1,3-diamine was synthesized by following a reported procedure.[1] Briefly, 4′-chloro- 2,2′:6′,2″-terpyridine, (300 mg, 1.12 mmol) was suspended in 1,3-diamino propane (2.16 ml). The reaction mixture was then refluxed at 120 °C for 10 h. After cooling to room temperature, distilled water (25 mL) was added, which has yielded a white precipitate. The white solid was further dissolved in dichloromethane and washed twice with distilled water. The organic layer was combined and dried over anhydrous Na_2SO_4. The solvent was removed under reduced pressure to yield a solid white product. Yield: 88%. ^{1}H-NMR (400 MHz, $CDCl_3$): δ: 8.53 (d, 2H, ArH), 8.52 (d, 2H, ArH), 7.76 (t, 2H, ArH), 7.60 (s, 2H, ArH), 7.25 (t, 2H, ArH), 5.16 (t, 1H, NH), 3.41 (m, 2H, $NHCH_2$), 2.84 (m, 2H, CH_2), 1.77 (m, 2H, NH_2CH_2). Selected FT-IR data (KBr, cm^{-1}): 3340 (b), 2965 (m), 1610-1560 (s), 1464 (m), 1402 (m), 1261 (m), 1094-981 (s), 791 (s). CHN analysis for $C_{18}H_{19}N_5$ Calc.: C, 70.81; H, 6.22; N, 22.95%. Expt.: C, 70.90; H, 6.11; N, 22.83%.

Step 2. Synthesis of TPY-ANT LMWG:

$ANT(COOH)_2$ (634 mg, 1.65 mmol) was dissolved in 50 ml of dry THF and $SOCl_2$ (2.4 ml, 33 mmol) was added into it under inert condition. The reaction mixture was refluxed for 2 hours at 65 °C. Then, the reaction mixture was distilled at 120 °C to remove excess $SOCl_2$ and yielded solid precipitate of acid chloride. Next, solid precipitate was dissolved in 40 ml of dry THF. Now, the solution of TPY-NH_2 (2.21 g, 7.26 mmol) in 10 ml of dry THF along with triethylamine (1.25 ml, 9 mmol) was added to the solution of acid chloride dropwise at 0 °C. The reaction was stirred at 0 °C for 12 hours. The solid precipitate was formed which was filtered and washed with chloroform and acetone to remove unreacted TPY-NH_2. The yield of isolated pale-yellow solid precipitate was found to be 48%. ^{1}H NMR (600 MHz, DMSO-d_6): δ = 8.78 (m, 2H), 8.66 (d, 4H, J= 6 Hz), 8.57 (m, 4H), 8.15 (d, 4H, J= 6 Hz), 7.95 (m, 4H), 7.74 (s, 4 H), 7.57 (m, 8H), 7.43 (m, 8H), 6.35 (broad, 2H), 3.53 (m, 4H), 1.98 (m, 4H), 1.26 (m, 4H). ^{13}C NMR{^{1}H} (150 MHz, DMSO-d_6): δ = 166.20, 155.99, 155.58, 154.99, 148.91, 137.00, 136.08, 130.90, 128.98, 127.59, 125.75, 123.82, 120.60, 105.65, 37.26, 35.37, 28.61. Selected FT-IR data (KBr, cm^{-1}): 3334 (s), 2920 (s), 2849 (s), 1652 (w), 1578 (s), 1484 (s), 1394 (m), 1314 (s), 1162 (m), 822 (w), 721 (s), 671 (m), 621(w), 530 (m), 490 (m), 440 (m). CHN analysis for $C_{64}H_{52}N_{10}O_2$ Calc.: C, 77.46; H, 5.82; N, 14.15 %; S: 6.78. Expt.: C, 77.40; H, 5.28; N, 14.10. MALDI-TOF: m/z calculated for $C_{64}H_{52}N_{10}O_2$: 992.4275; found: $[M+H]^+$ 993.4276.

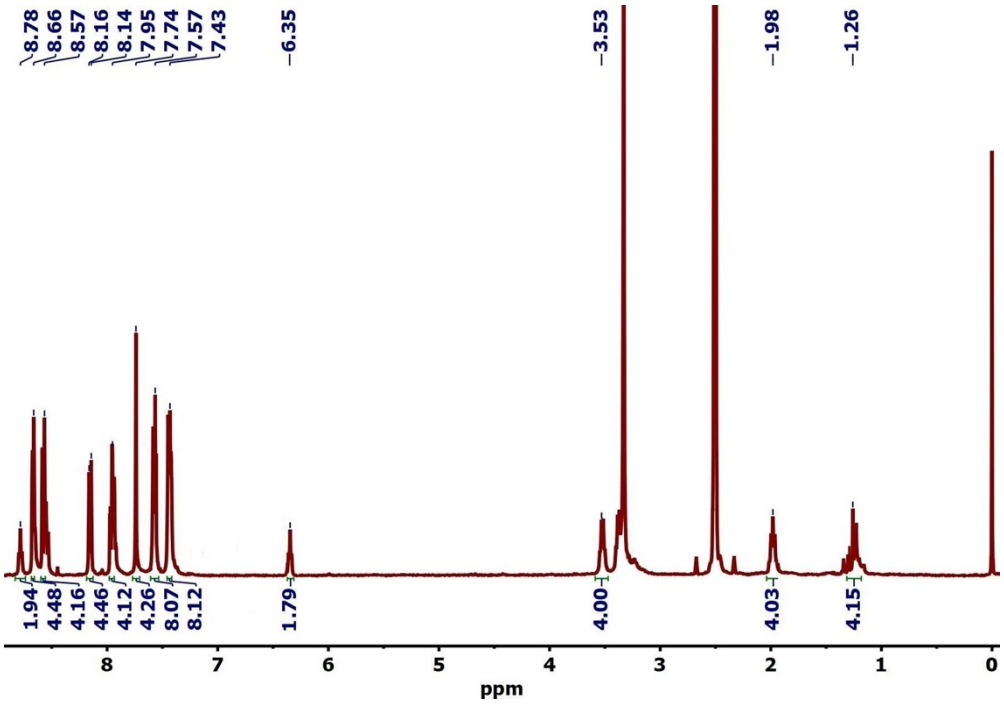

Figure S1: ^{1}H NMR of TPY-ANT LMWG in DMSO-d_6.

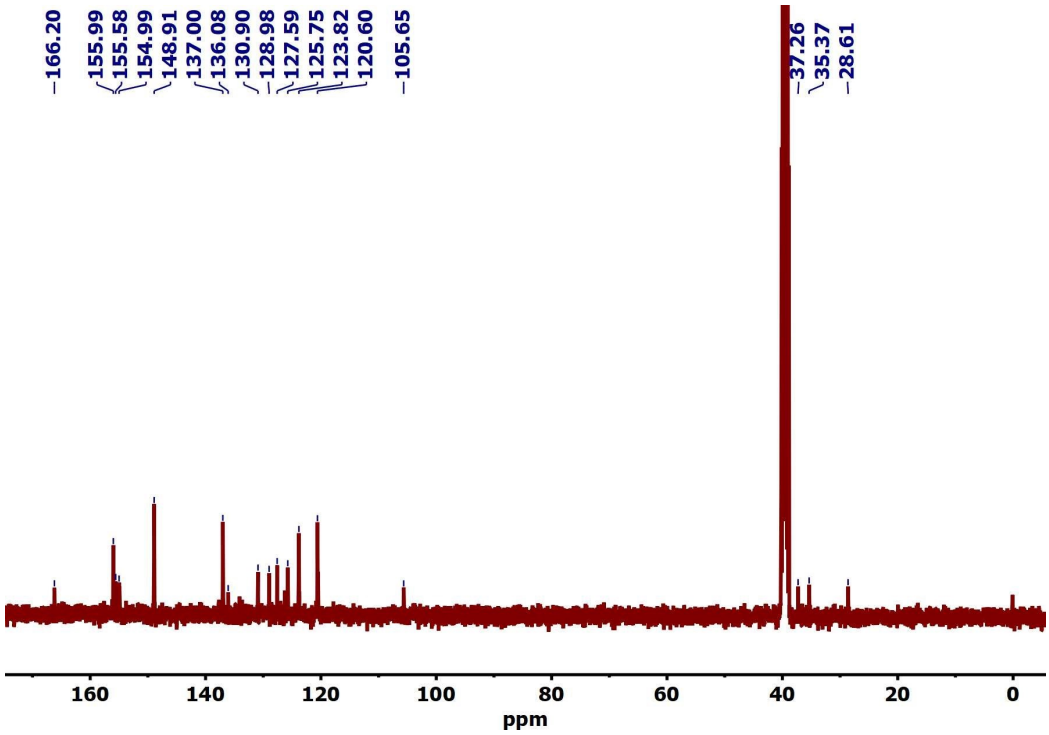

Figure S2: ^{13}C NMR of TPY-ANT LMWG in DMSO-d_6.

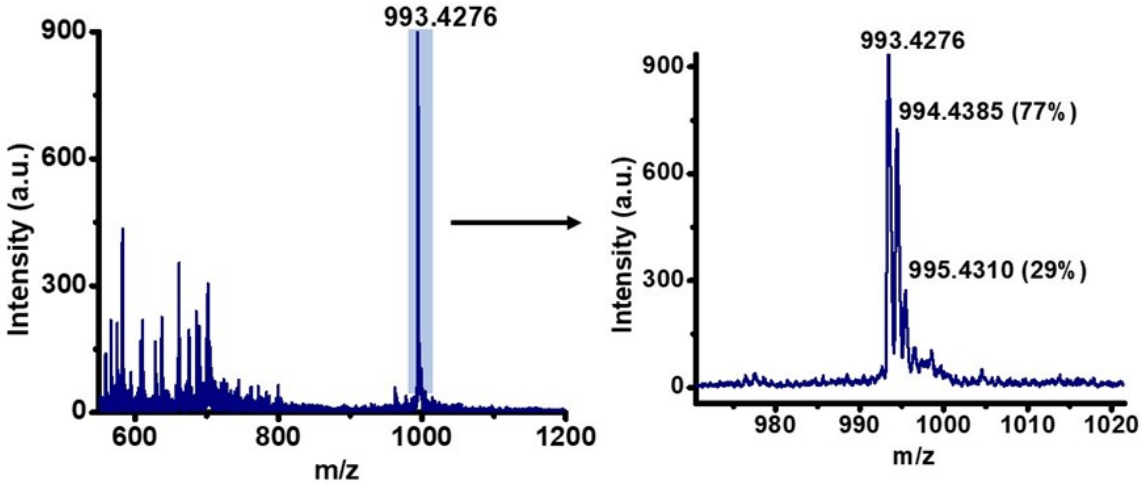

Figure S3: HR-MS of TPY-ANT LMWG.

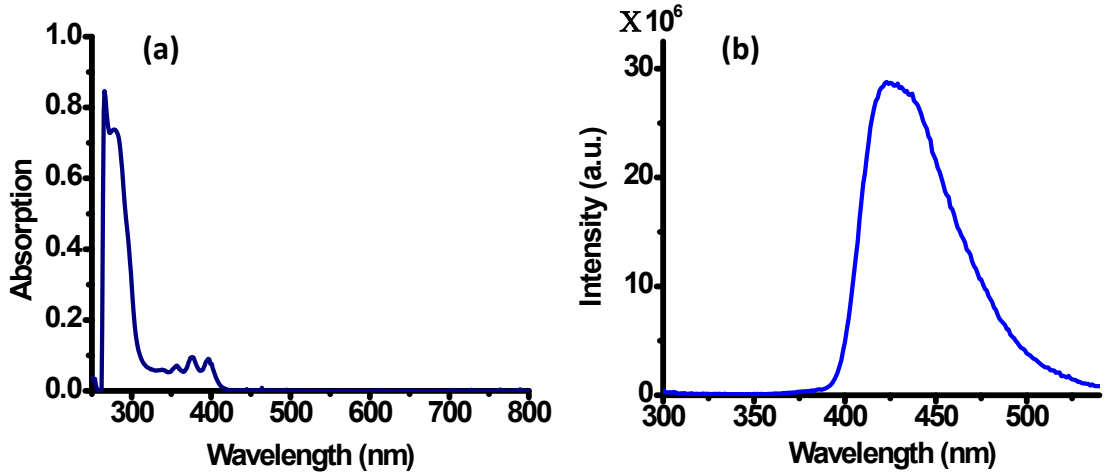

Figure S4: (a) UV-Vis absorption spectrum and (b) Emission spectrum for TPY-ANT LMWG (2 × 10^{-5} M in DMF).

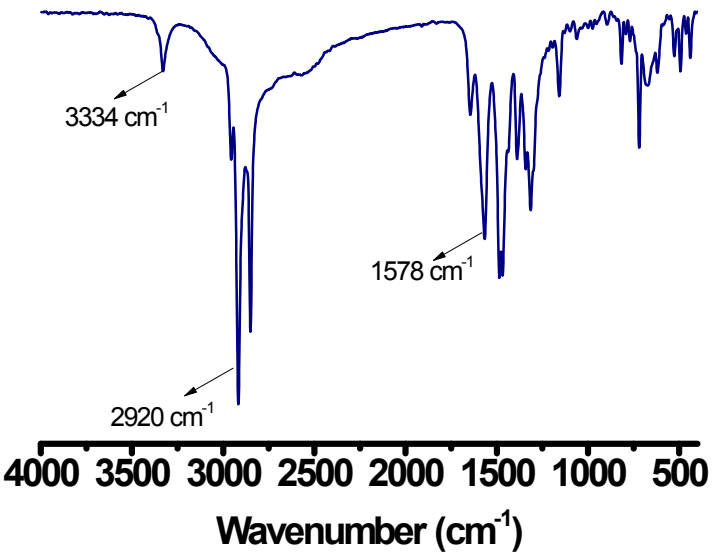

Figure S5: FT-IR spectrum for TPY-ANT LMWG.

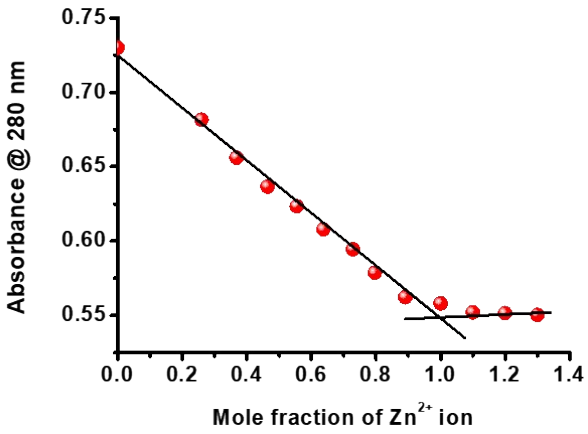

Figure S6: Job's plot analysis for TPY-ANT LMWG (2 x 10^{-5} M) with Zn^{2+} in DMF (binding stochiometric ratio of TPY-ANT: Zn^{2+} is 1:1).

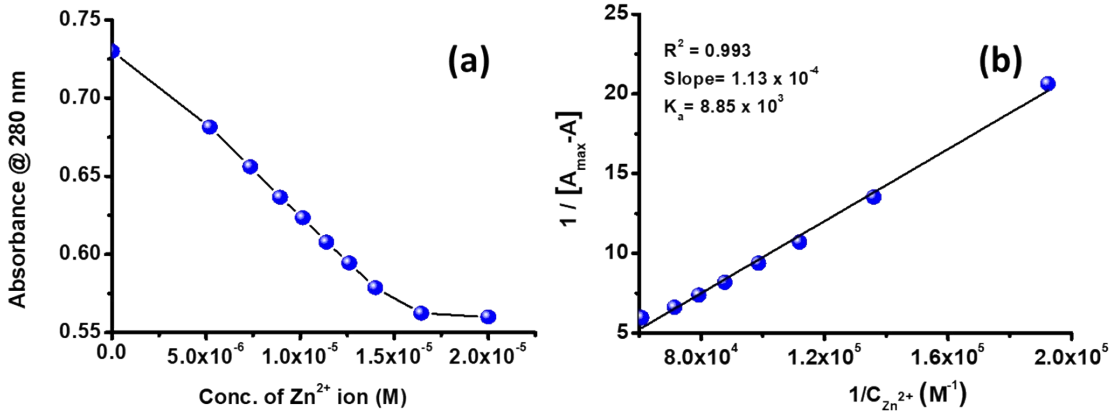

Figure S7: (a) Change in absorption at 280 nm with addition of Zn^{2+} and (b)Benesi-Hildebrand plot obtained from the titration experiment of TPY-ANT LMWG (2 × 10^{-5} M in DMF) with Zn^{2+} (5 × 10^{-4} M in DMF: stock solution).

Table S1: Gelation ability of TPY-ANT LMWG in different conditions:

No.	CPG formation; **TPY-ANT + Zn^{2+} ion (1:1 molar ratio)**	**Solvent Ratio**	Heating/Cooling	**Gelation ability**
1.	TPY-ANT (DMF) + Zn^{2+} (DMF)	(1:1)	80°/15° C	Solution
2.	TPY-ANT (DMF) + Zn^{2+} (H_2O)	(2:1)	80°/15° C	Solution
3.	TPY-ANT (DMF) + Zn^{2+} (H_2O)	(1:1)	80°/15° C	Dispersion
4.	TPY-ANT (DMF) + Zn^{2+} (H_2O)	(1:2)	80°/15° C	Dispersion
5.	TPY-ANT (DMF) + Zn^{2+} (H_2O)	(1:3)	80°/15° C	**Gel***
6.	TPY-ANT (DMF) + Zn^{2+} (H_2O)	(1:4)	80°/15° C	Precipitate

*CGC (Critical Gelator Concentration) = 0.005 mmol; DMF= Dimethylformamide.

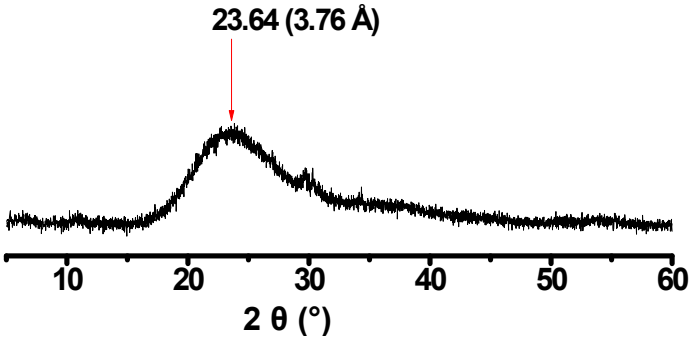

Figure S8: PXRD pattern analysis for Zn-TPY-ANT CPG.

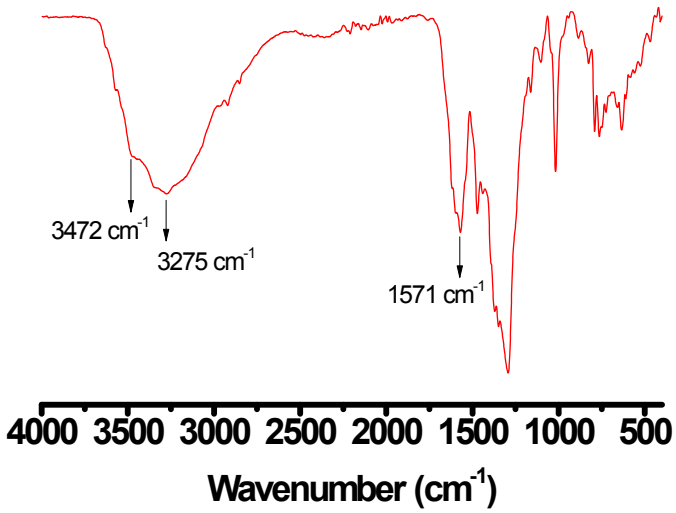

Figure S9: FT-IR spectrum for Zn-TPY-ANT CPG.

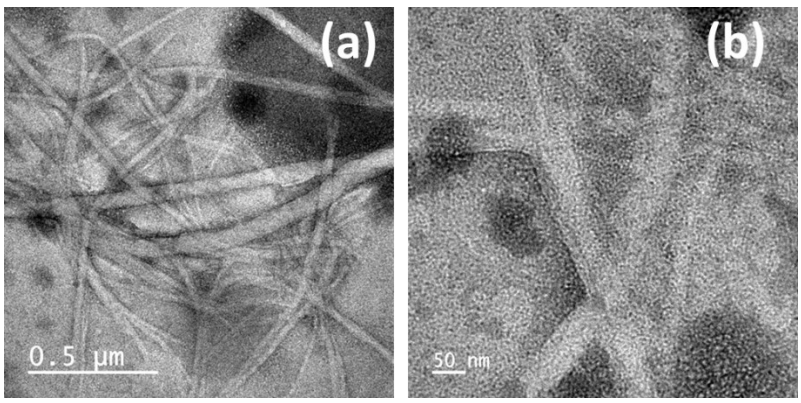

Figure S10: TEM image of Zn-TPY-ANT in gel state. (a) at low resolution and (b) at high resolution. (dark spots could be due to beam damage).

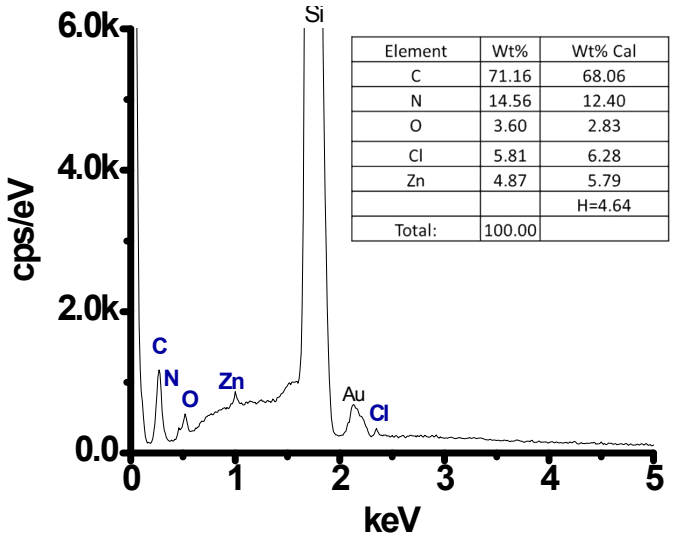

Element	Wt%	Wt% Cal
C	71.16	68.06
N	14.56	12.40
O	3.60	2.83
Cl	5.81	6.28
Zn	4.87	5.79
		H=4.64
Total:	100.00	

Figure S11: EDAX analysis for Zn-TPY-ANT CPG (as-synthesized xerogel).

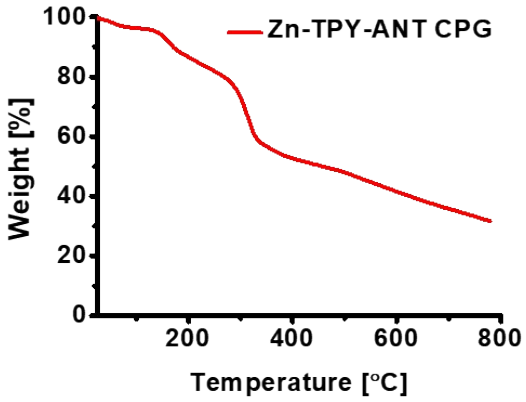

Figure S12: TGA for Zn-TPY-ANT CPG.

S3. Electrochemical characterizations:

(a) Mott–Schottky measurement

The energy band structure of TPY-ANT OG and Zn-TPY-ANT CPG was depicted by the Mott Schottky (MS) analysis (at 2000 Hz, from -2.0 V to +2.0 V) using ITO as a working electrode (WE) in the N_2-purged aqueous solution of 0.2 M Na_2SO_4 at pH=7, Pt as a counter electrode (CE) and Ag/AgCl as a reference electrode (RE). The curve was fitted by Eq. 1.[2] An electrochemical ink was prepared by making a dispersion of a mixture of catalyst (2.0 mg) in the solvent mixture of isopropanol (500 µl), water (500 µl), and Nafion (14 µl). Upon sonication for 20 minutes, a well-dispersed ink (3.5 µl) was drop cast over the ITO electrode and allowed to dry for 3 h under ambient conditions.

$$1/C^2 = (2/\varepsilon \varepsilon_0 A^2 e N_D)(E-E_{FB} - k_B T/e) \quad \text{…….. Eq.1}$$

Where, C and A are the interfacial capacitance and area, respectively. ε is the dielectric constant of the semiconductor, and ε_0 is the permittivity of free space. k_B Boltzmann constant, T the absolute temperature, and e is the electronic charge. N_D the number of donors, V the applied voltage. Therefore, a plot of $1/C^2$ against V should yield a straight line from which V_{fb} can be determined from the intercept on the V axis.

Calculation of Conduction Band (E_{CB}) and Valance Band (E_{VB}) versus RHE (at pH=7):

The conduction band edge (CB_{Edge}) potentials for Zn-TPY-ANT CPG and TPY-ANT OG were assigned based on flat band potentials and valance band (VB) position was calculated by using equation 2.

$E_{VB} = E_{CB\ Edge}$ + Band Gap …….. Eq. 2

(i) Zn-TPY-ANT CPG

$E_{CB\ Edge\ (\textbf{Zn-TPY-ANT\ CPG})} = V_{fb} = -0.44$ V

$E_{VB\ (\textbf{Zn-TPY-ANT}\ CPG)} = -0.44 + \text{Band Gap}_{\textbf{(Zn-TPY-ANT CPG)}} = -0.44 + 2.30 = 1.86$ V

(ii) For TPY-ANT OG

$E_{CB\ Edge\ (\textbf{TPY-ANT}\ OG)} = V_{fb} = -0.58$ V

$E_{VB\ (\textbf{TPY-ANT}\ OG)} = -0.58 + \text{Band Gap}_{\textbf{(TPY-ANT OG)}} = -0.58 + 2.85 = 2.27$ V

(b) Photocurrent Measurement

A similar setup was used for photocurrent measurements as employed for Mott-Schottky analysis. Here, the photocurrent study was performed for TPY-ANT OG and Zn-TPY-ANT CPG upon consecutive light "ON-OFF" for 30 s over 10 cycles at + 0.5 V.

(c) Electrochemical Impedance analysis and cyclic voltammetry:

Electrochemical Impedance Spectroscopy (EIS) and cyclic voltammetry (CV) were performed in a three-electrode cell configuration with a glassy carbon electrode as the working electrode (WE), platinum as a counter electrode (CE), and Ag/AgCl as a reference electrode (RE). For EIS measurements, 0.2 M Na_2SO_4 was used as an electrolyte at pH = 7. An electrochemical ink was prepared by making a dispersion of a mixture of xerogel state of catalyst (1.0 mg) in the solvent mixture of isopropanol (500 µl) and water (500 µl). Upon sonication for 30 minutes, a well-dispersed ink (3.5 µl) was drop cast over the GC electrode and allowed to dry for 3 h under ambient conditions. EIS was recorded at -1.2 V_{RHE} applied bias from 0.1 Hz to 100 kHz (under the dark condition and visible light irradiation). CV was recorded for xerogel of catalyst

in 0.2 M Na_2SO_4 aqueous solution using similar three electrode setup as for EIS. Further, the pH=12 was adjusted by 5 vol % of TEA addition in the electrolyte.

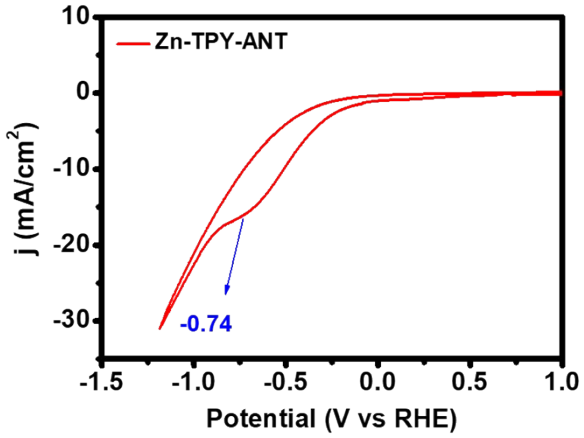

Figure S13: Cyclic voltammogram of Zn-TPY-ANT xerogel at pH=12.

S4. Photocatalytic water reduction experiments:

Photocatalytic H_2 evolution experiments were carried out in a 30 mL borosilicate glass cell containing a magnetic stir bar sealed with a septum. For the photocatalytic experiment, 5 mg of gel catalyst was dispersed in 8 mL water containing 0.4 ml of triethylamine (TEA) as a sacrificial agent. Whereas, the photocatalytic experiments for xerogel state of catalyst were carried out from 1 mg of sample dispersion in 10 ml water along with 0.5 ml of TEA as sacrificial electron donor. The suspensions were ultrasonicated for 20 minutes to make a homogeneous dispersion. The reaction mixture was then purged with N_2 for 30 minutes to remove any traces of dissolved H_2 gas and air, which was ensured by GC-analysis before performing the photocatalysis. The reaction mixture was irradiated with a 300 W Xe lamp (Newport) fitted with a 10 cm (Intensity 1.5 Sun) path length of water filter for removal of IR radiation. A visible bandpass filter (400 nm–750 nm) was used to block the UV light. The Headspace gases were sampled using Hamilton air-tight syringes by injecting 250 µL into the gas chromatograph (Agilent CN15343150). Referencing of the gas chromatography was done against a standard (H_2/N_2) gas mixture with a known concentration of hydrogen for the calibration curve, where N_2 was used as a carrier gas and a thermal conductivity detector (TCD) was used for H_2 detection. Notably, negligible hydrogen evolution was observed for TEA aqueous solution (0.35 mol/L) under visible light irradiation in the absence of a photocatalyst. Under similar conditions the photocatalytic experiments were performed in presence of different sacrificial agent (0.35 mol/L).

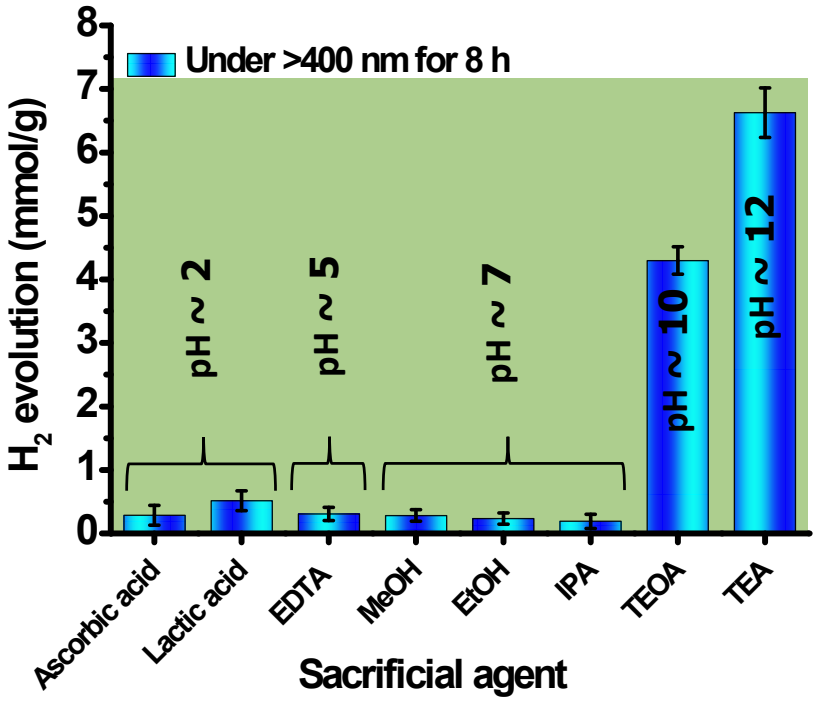

Figure S14: Photocatalytic H_2 production experiments using different sacrificial electron donors for Zn-TPY-ANT catalyst (0.35 mol/L sacrificial electron donor and 5 mg of gel catalyst was taken in aqueous medium in each experiments). Light was irradiated for 8 h using visible band pass filter (>400 nm).

Quantum efficiency measurements

The quantum efficiency is defined by the ratio of the effective electron used for product formation to the total input photon flux.

$$QE\% = \left[\frac{Effective\ electrons}{Total\ photons}\right] \times 100\% = \left[\frac{n \times Y \times N}{\theta \times T \times S}\right] \times 100\%$$

Where n is the number of electrons used in the photocatalysis process (n=2), Y is the yield of evolved gas from the sample (mol), N is the Avogadro's number (6.022×10^{23} mol^{-1}), θ is the photon flux, T is the irradiation time, and S is the illumination area (12.56 cm^2). The photon flux was calculated at 400 ± 5 nm by using the bandpass filter with the help of a power meter (Coherent; Model: LaserCheck 1098293).

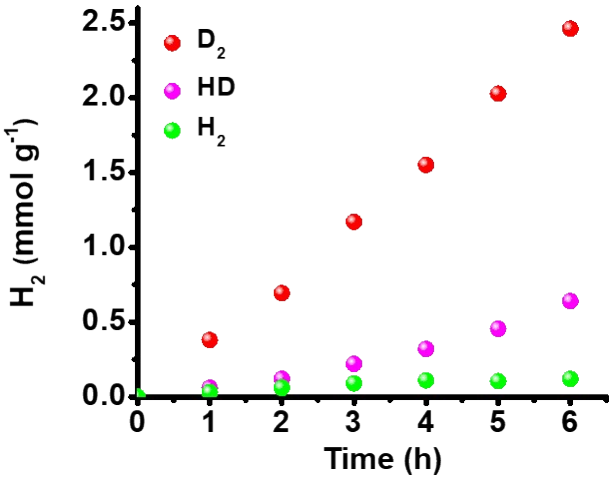

Figure S15: Photocatalytic gas evolution using Zn-TPY-ANT xerogel (1 mg) from a D_2O/triethylamine mixture (95:5) under visible light irradiation (300 W Xe light source, $\lambda >$ 400 nm). The high relative rate of D_2 production compared to HD and H_2 (D_2: 70%, HD: 28%, and H_2: 2%) is clearly indicated that the water reduction is the origin of the gas evolution. HD and H_2 as side-products potentially originate from the H-D exchange between D_2O and triethylamine or from water that was present in the triethylamine.

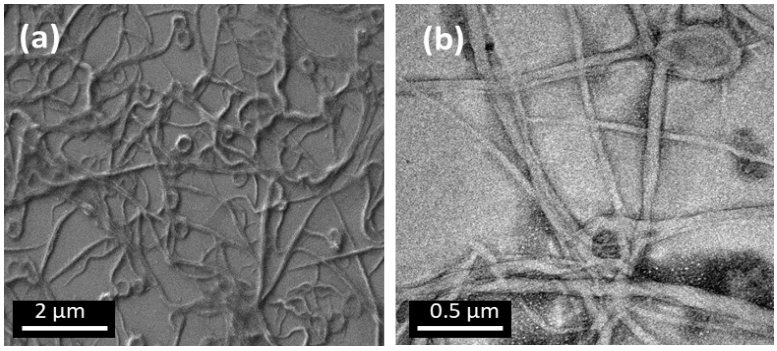

Figure S16: (a) FE-SEM and (b) TEM after photocatalysis (>290 nm) for Zn-TPY-ANT.

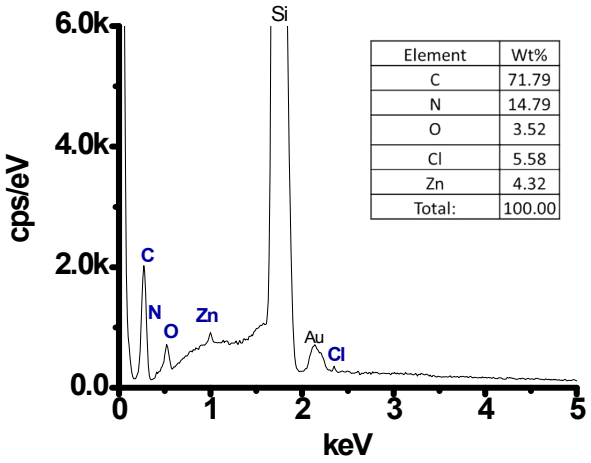

Figure S17: EDAX analysis for Zn-TPY-ANT (after photocatalysis (>290 nm) sample was collected and washed with water).

Table S2. Comparison table of the H_2 evolution of Zn-TPY-ANT with some of the reported hybrid materials under visible light irradiation.

S. No.	Catalyst	Reaction medium	activity for H_2	Ref
1.	**Zn-TPY-ANT CPG**	**H_2O/TEA**	**0.97 mmol g^{-1} h^{-1}**	**This work**
2.	N_2-COF/ chloro(pyridine) cobaloxime co-catalyst	H_2O, acetonitrile/ TEOA	0.78 mmol g^{-1} h^{-1}	*J. Am. Chem. Soc.* **139**, 16228-16234 (2017)
3.	Thiazolo[5,4-d]thiazole-COF (TpDTz)+ Ni- cluster co-catalyst	H_2O/ TEOA	0.94 mmol g^{-1} h^{-1}	*J. Am. Chem. Soc.* **141**, 11082-11092 (2019)
4.	1 wt % Pt-loaded WO_x NWs	H_2O/ MeOH	0.46 mmol g^{-1} h^{-1}	*ACS Energy Lett.*, **3**, 1904−1910 (2018)
5.	PB2S (conjugated organoborane oligomers)	H_2O/ TEA	0.22 mmol g^{-1} h^{-1}	*ACS Energy Lett.*, **5**, 669-675 (2020)
6.	TP-BDDA COF + Pt co-catalyst	H_2O/ TEOA	0.32 mmol g^{-1} h^{-1}	*J. Am. Chem. Soc.*, **140**, 1423−1427 (2018)
7.	Tetraphenylethylene (TPE) Based CMP	H_2O/ MeOH/ Na_2S, Na_2SO_4	0.65 mmol g^{-1} h^{-1}	*Chem. Eur. J.* **25**, 3867 – 3874 (2019)
8.	PTCDIs- C_3N_4 aggregates/ Pt NP	H_2O/ TEOA	3.8 μmol h^{-1}	*Appl. Catal., A* **498**, 63–68 (2015).

9.	PBI-F gel/ 1 mol % PVP capped Pt	H_2O/ MeOH	3.0 μmol g^{-1} h^{-1}	*J. Mater. Chem. A* **5**, 7555-7563 (2017)

S5. Synthesis and characterization of TPY-ANT organogel: As a control experiment, the organogel was synthesized by adapting the reported procedure.[1] In brief, 1×10^{-3} M TPY-ANT solution in 1:1 $CHCl_3$/THF mixture was heated at 90 ºC for few minutes in a closed vial to form a viscous liquid which on cooling results in the opaque gel. The formation of the gel was confirmed by inversion-test as well as rheology studies. TPY-ANT organogel (OG) also showed the LVE (G′ > G″) region in the strain range from 0.01% to 1%, this indicated the stable gel formation.

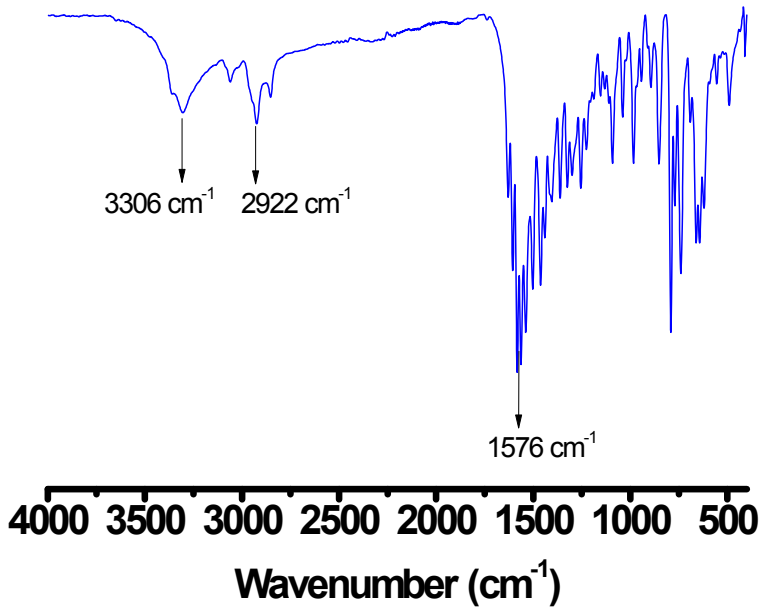

Figure S18: FT-IR spectrum for TPY-ANT organogel.

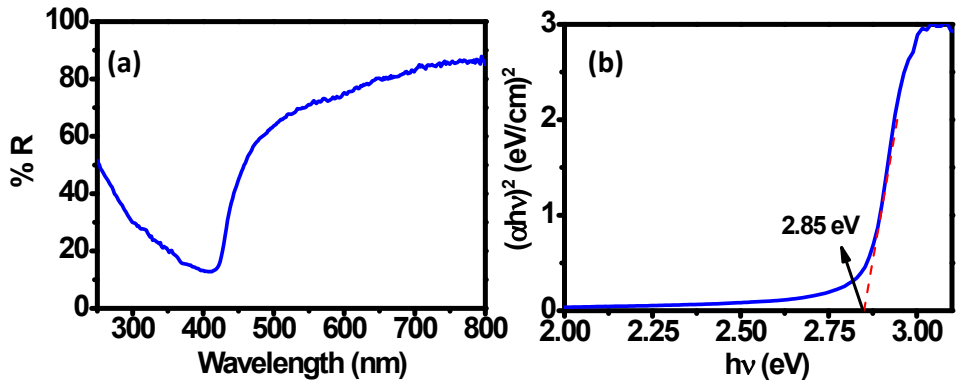

Figure S19: (i) Reflectance spectra of TPY-ANT OG. (ii) Tauc plot for bandgap calculation of TPY-ANT organogel.

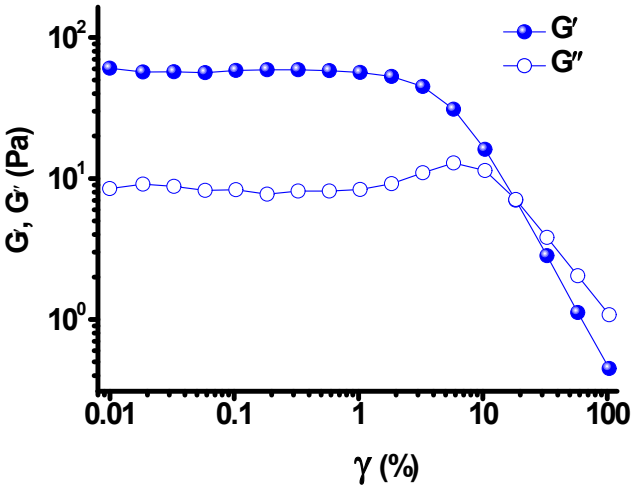

Figure S20: Strain-sweep rheology data for TPY-ANT organogel at 25° C.

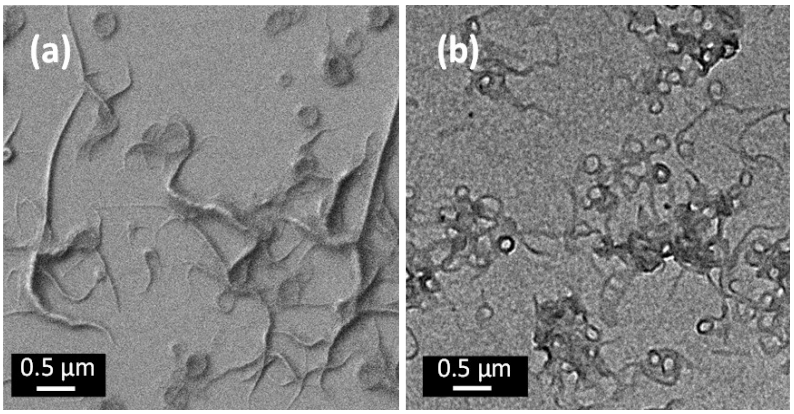

Figure S21: (a) FESEM image and (b) TEM images of TPY-ANT organogel showing the presence of nanofibers and nanoring.

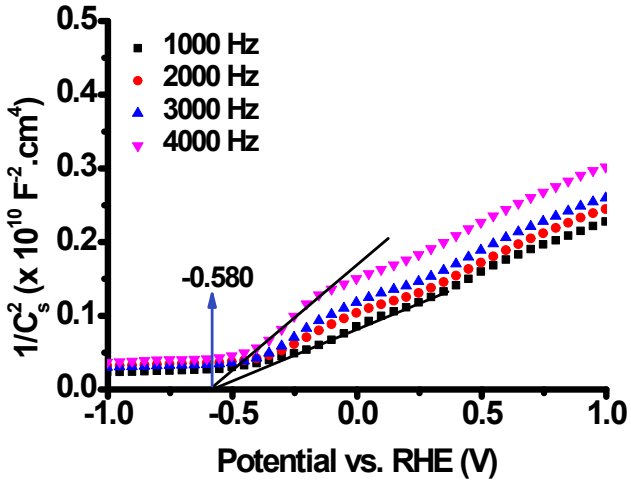

Figure S22: Mott-Schottky analysis for TPY-ANT xerogel.

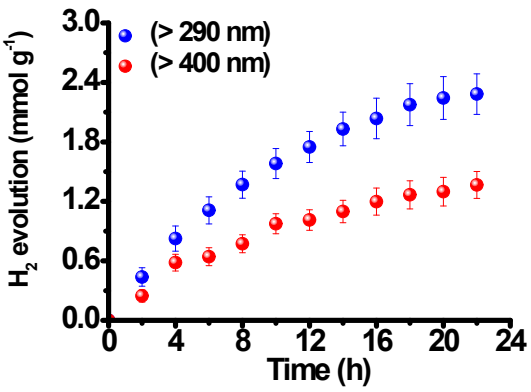

Figure S23: Photocatalytic H_2 production experiment for TPY-ANT. (5 mg gel of catalyst was well dispersed in 4 ml of water with 2 vol % TEA).

S6. Synthesis of ANT-Zn Coordination Polymer (ANT-Zn-CP): Unit formula = $[Zn(ANT)(DMF)_2]_n$: Synthesis was done by following a reported literature procedure.[3] In a 15 ml vial, $Zn(NO_3)_2.6H_2O$ (33 mg, 0.11 mmol) and DMF (2.5 ml) were combined. The reaction was subjected to ultra-sonification for 5 min, followed by the addition of 4,4′-(anthracene-9,10-diyl)dibenzoic acid (29 mg, 0.07 mmol). Trifluoroacetic acid (37 µl) was added as a modulator, and the vial was sealed and subjected to ultra-sonification for an additional 30 min. The vial was then placed at 120°C for 12 hours. The solution was cooled and the resulting solids were isolated by centrifugation, followed by washing with dichloromethane and drying. The pale yellow coloured microcrystalline product was obtained.

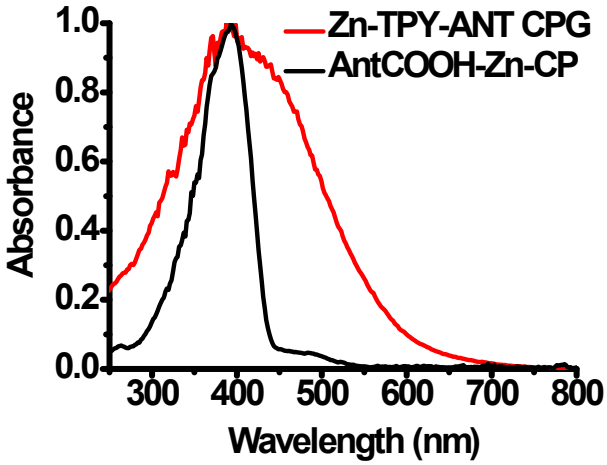

Figure S24: Comparison of UV-Visible absorption spectrum for Zn-TPY-ANT CPG and ANT-Zn-CP.

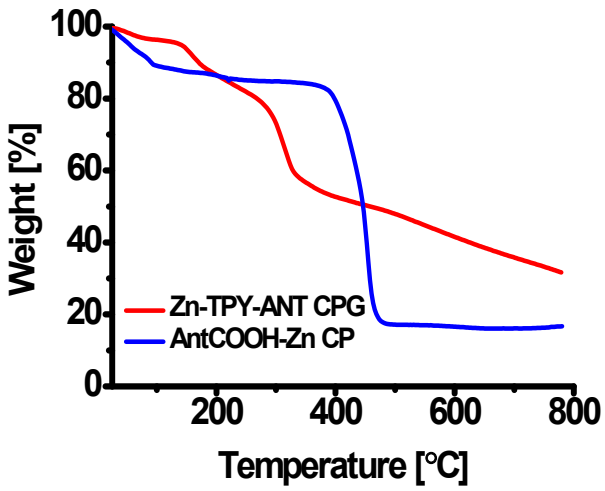

Figure S25: Comparison of TGA analysis for Zn-TPY-ANT CPG and ANT-Zn-CP.

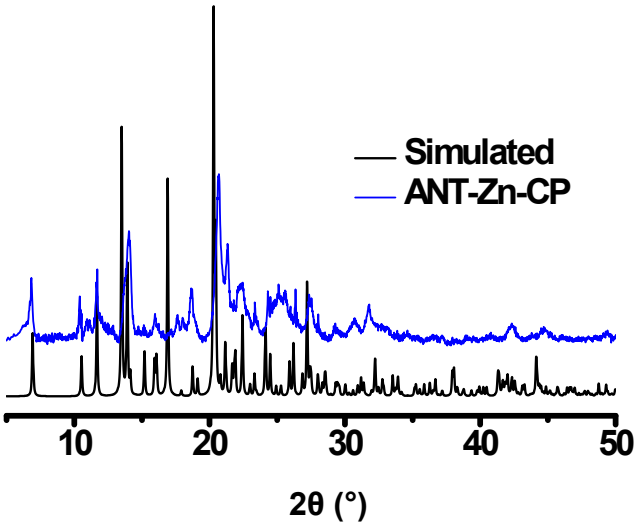

Figure S26: X-ray diffraction data for microcrystalline ANT-Zn-CP.

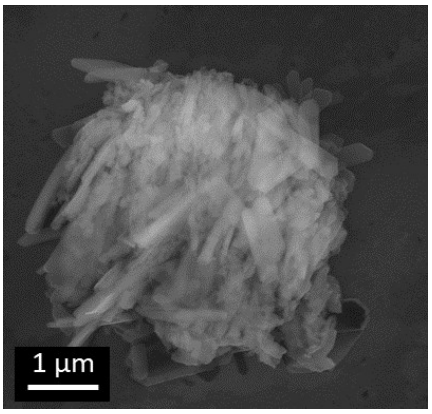

Figure S27: FESEM image of microcrystalline ANT-Zn-CP**.**

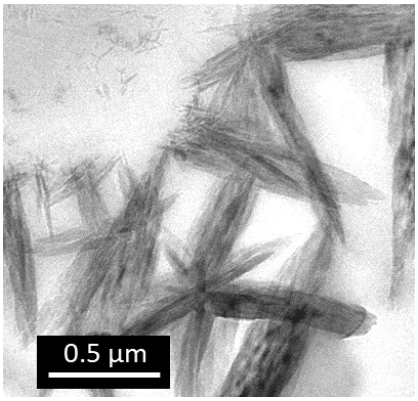

Figure S28 TEM image of microcrystalline ANT-Zn-CP.

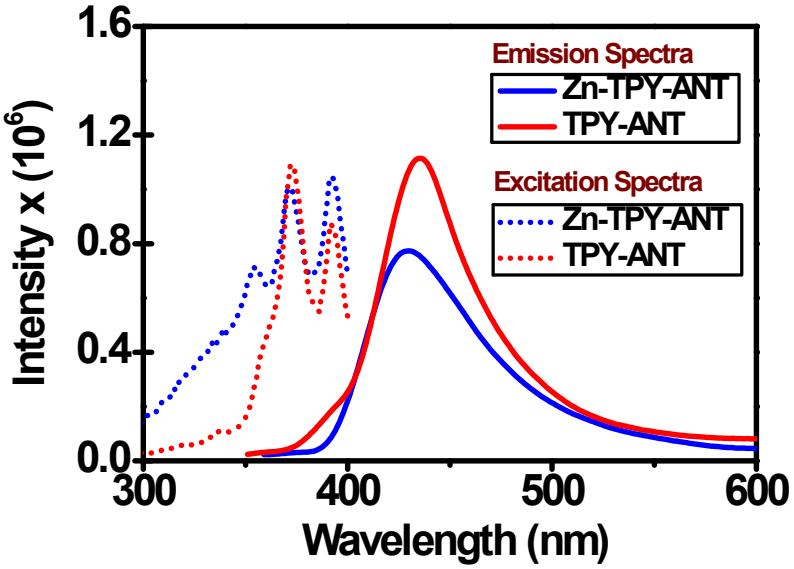

Figure S29. Excitation and emission spectra for TPY-ANT OG and Zn-TPY-ANT CPG (the thin film of gel-coated quartz plate for the measurement: λ_{excit} = 390 nm; λ_{em} (TPY-ANT OG) = 435 nm and λ_{em} (Zn-TPY-ANT CPG) = 425 nm).

Lifetime calculations: The lifetime data for TPY-ANT OG and Zn-TPY-ANT CPG were collected upon exciting at 390 nm and corresponding decay was collected at 425 nm. The average lifetime is calculated using the following formula:

Average life time, τ_{avg}(ns) = ($\Sigma A_i\tau_i^2/\Sigma A_i\tau_i$)

Where, τ_{avg} = average lifetime in nano-seconds, ΣA_i = sum of the percentage of all the components exists in the excited state, $\Sigma\tau_i$ = sum of the excited-state lifetime of all the component.

Table S3. Lifetime data:

Sample	τ_1 **(ns)**	A1	τ_2 **(ns)**	A2	τ_{av} **(ns)**
TPY-ANT OG	38.8	37.54 %	8.7	62.46 %	**30.6**
Zn-TPY-ANT CPG	3.97	97.82 %	9.9	2.18 %	**4.28**

S7. Computational (DFT) details: All the electronic structure calculations were performed under the Density functional theory (DFT) model using the Gaussian 16 package of programs.[4] DFT calculations were performed to reveal the feasibility of photoinduced electron transfer from light-harvesting anthracene moiety (Table S4) to zinc terpyridine unit (Table S5). Molecular geometries were optimized using B3LYP-D3[5-10] exchange-correlation functional. For geometry optimization typically 6-31+G(d) basis set was used for all atoms (HCNOCl) except Zn, for which LANL2DZ valence basis set,[11-13] which uses a widely used effective core potential (ECP), was used. In computations, the implicit solvent effect of water was considered by the polarizable continuum model (PCM).[14] The optimized structures were subjected to harmonic vibrational frequency analysis to check the nature of the stationary points. Later, the optimized structures were put into single point energy calculation using a higher basis set 6-311++G(d,p) for all lighter atoms (HCNOCl) whereas LANL2DZ for Zn to bring in more accuracy. All the molecular orbital diagrams were generated using an isovalue of 0.04 from GaussView 6.0.16.[15]

Table S4. DFT-optimized geometry of anthracene (singlet), computed at the B3LYP-D3/ 6-31+G(d) (HCNO) level in water solvent using PCM model.

Atom	x	y	z
C	-2.07565100	-3.11103900	0.07037400
C	-0.75027600	-2.75566600	0.06560200
C	-2.74764600	-0.77946100	0.09193200
C	-0.34664800	-1.37900700	0.07619300
C	-3.08886000	-2.10855500	0.08748900
C	-1.37538000	-0.36116800	0.08081000
C	1.01371700	-1.00305800	0.07855500
C	1.37538000	0.36116800	0.08081000
C	2.74764600	0.77946100	0.09193200
C	0.34664800	1.37900700	0.07619300
C	-1.01371700	1.00305800	0.07855500
C	3.08886000	2.10855500	0.08748900
C	2.07565100	3.11103900	0.07037400
C	0.75027600	2.75566600	0.06560200
C	-2.07565100	2.05491200	0.08043900
C	-4.07616400	4.04504800	0.08440600
C	-2.50023300	2.63980600	1.28341300
C	-2.67077000	2.47172300	-1.11868000
C	-3.65799600	3.45858600	-1.12012100
C	-3.49455200	3.61680100	1.28674600
C	2.07565100	-2.05491200	0.08043900
C	4.07616400	-4.04504800	0.08440600
C	2.50023300	-2.63980600	1.28341300
C	2.67077000	-2.47172300	-1.11868000
C	3.65799600	-3.45858600	-1.12012100
C	3.49455200	-3.61680100	1.28674600
C	-5.14457000	5.09927000	0.15003800
C	5.14457000	-5.09927000	0.15003800
O	-5.87143100	5.22187200	1.15077200
O	5.87143100	-5.22187200	1.15077200
N	5.27867700	-5.90524800	-0.93028200
N	-5.27867700	5.90524800	-0.93028200
C	6.27606400	-6.96667800	-0.97798900
C	-6.27606400	6.96667800	-0.97798900

H	7.26918100	-6.55829100	-0.76982800
H	6.26929900	-7.40479100	-1.97749600
H	6.06075300	-7.74762800	-0.23919800
H	4.58082300	-5.87459500	-1.66096000
H	4.11728300	-3.74173500	-2.06319000
H	2.36278700	-2.01525100	-2.05560400
H	0.01520600	-3.52462100	0.05352900
H	2.04747900	-2.32417900	2.21971500
H	3.82544900	-4.06005300	2.22080100
H	-2.35742400	-4.16061700	0.06211600
H	-4.13537700	-2.40146600	0.09632600
H	-3.52474900	-0.02228000	0.10434300
H	-2.04747900	2.32417900	2.21971500
H	-3.82544900	4.06005300	2.22080100
H	3.52474900	0.02228000	0.10434300
H	4.13537700	2.40146600	0.09632600
H	2.35742400	4.16061700	0.06211600
H	-0.01520600	3.52462100	0.05352900
H	-2.36278700	2.01525100	-2.05560400
H	-4.11728300	3.74173500	-2.06319000
H	-6.06075300	7.74762800	-0.23919800
H	-4.58082300	5.87459500	-1.66096000
H	-6.26929900	7.40479100	-1.97749600
H	-7.26918100	6.55829100	-0.76982800

Table S5. DFT-optimized geometry of $Zn(TPY)_2Cl_2$ (singlet), computed at the B3LYP-D3/ LANL2DZ (Zn)/ 6-31+G(d) (HCNCl) level in water solvent using PCM model.

Atom	x	y	z
C	7.06310400	-1.05794100	-0.53692400
H	6.83821900	-2.11811200	-0.36722400
H	6.93491900	-0.83524000	-1.60338000
C	4.87073400	-0.16197400	0.22121200
C	4.14024500	-0.97605200	-0.68063900
C	4.13593600	0.70973800	1.06788800

C	2.75405500	-0.88496500	-0.70183600
H	4.66090100	-1.65608200	-1.34010100
C	2.75412800	0.73182900	0.98642000
H	4.67083900	1.34633100	1.76286700
C	1.88924900	-1.68642300	-1.62186700
C	2.39290200	-2.58449500	-2.56935500
C	1.50180800	-3.27580000	-3.39147500
H	3.45888700	-2.74650000	-2.67466900
C	-0.29393400	-2.14971100	-2.28236600
C	0.13056900	-3.05902000	-3.25046400
H	1.87801700	-3.97547800	-4.13153000
H	-1.34781800	-1.93838500	-2.12429000
H	-0.59406800	-3.57863600	-3.86803800
C	1.88547500	1.59926100	1.83936400
C	2.37965400	2.43672500	2.84578800
C	-0.29852400	2.25070000	2.31324500
C	1.48352200	3.19606200	3.59901300
H	3.44179500	2.49774100	3.05035300
C	0.11647300	3.10619900	3.33267200
H	-1.34860400	2.13793200	2.05824100
H	1.85225400	3.84937300	4.38386200
H	-0.61153900	3.68183200	3.89403700
N	6.22140900	-0.20150800	0.28583900
H	6.67864500	0.40480100	0.95316500
N	2.08333100	-0.05117300	0.11410400
N	0.55902300	-1.48351800	-1.49492600
N	0.55925100	1.51909700	1.59114400
Zn	-0.03997700	0.05205400	0.01713100
C	-2.92011600	-0.64326900	0.66452400
C	-2.74148200	0.95957500	-1.02749700
C	-4.30747900	-0.63696300	0.59023000
C	-4.11723700	1.03107200	-1.16524600
C	-4.94360700	0.21755800	-0.34522300
H	-4.89966100	-1.27276900	1.23336600
H	-4.57826300	1.69491500	-1.88731300
C	-2.14957300	-1.49814000	1.61955300
C	-2.75090400	-2.34732300	2.55497200
C	-0.03085500	-2.11505100	2.36038600
C	-1.94261100	-3.09379900	3.41384700
H	-3.82894400	-2.42966400	2.62339300

C	-0.55501600	-2.97972100	3.32057900
H	1.04068700	-1.98540000	2.23690800
H	-2.39546700	-3.75598500	4.14544100
H	0.10726900	-3.54446400	3.96780500
C	-1.78204200	1.76342100	-1.84468400
C	-2.17917800	2.65900200	-2.84388400
C	0.45987200	2.23882200	-2.25261300
C	-1.20406300	3.35485900	-3.55977800
H	-3.22717000	2.81606100	-3.06881800
C	0.14359100	3.14510400	-3.26374400
H	1.48984000	2.03417600	-1.97426700
H	-1.49747900	4.05243800	-4.33830700
H	0.93105200	3.66855100	-3.79510600
N	-0.80413900	-1.39633700	1.53766400
N	-2.16153100	0.13570900	-0.12829200
N	-0.47380100	1.56845000	-1.56647600
N	-6.29014800	0.26827600	-0.46570400
H	-6.67790100	0.90179400	-1.15130600
H	8.10414200	-0.87596200	-0.26686300
C	-7.22124800	-0.52565800	0.32262500
H	-8.23532500	-0.27941200	0.00509700
H	-7.05784800	-1.59931500	0.16805700
H	-7.12671000	-0.30385500	1.39276900
Cl	0.67021300	5.77857100	0.06966000
Cl	0.07709300	-5.69663100	0.09505400

S7. References:

1. Sutar, P.; Suresh, V. M.; Maji, T. K., *Chem. Commun*. 2015, **51**, 9876-9879.
2. Gelderman, K.; Lee, L.; Donne, S. W., *J. Chem. Edu.* 2007, 84, 685.
3. Amemori S., Gupta R. K., Bohm M. L., Xiao J., Huynh U., Oyama T., Kaneko K., Rao A., Yanai N., Kimizuka N., *Dalton Trans*., 2018, **47**, 8590-8594.
4. M. J. Frisch, G. W. Trucks and H. B. Schlegel, 2009.
5. K. Kim and K. D. Jordan, *J. Phys. Chem.,* 1994, **98**, 10089-10094.
6. P. J. Stephens, F. J. Devlin, C. F. Chabalowski and M. J. Frisch, *J. Phys. Chem*., 1994, **98**, 11623-11627.
7. A. D. Becke, *Phys. Rev. A*., 1998, **38**, 3098-3100.
8. Chengteh Lee, Weitao Yang and Robert G. Parr, *Phys. Rev. B*., 1988, **37**, 785-789.

9. S. H. Vosko, L. Wilk and M. Nusair, *Can. J. Phys*., 1980, **58**, 1200-1211.
10. A. D. Becke, *J. Chem. Phys*., 1993, **98**, 5648-5652.
11. W. R. Wadt and P. J. Hay, *J. Chem. Phys.,* 1985, **82**, 270.
12. W. R. Wadt and P. J. Hay, *J. Chem. Phys.,* 1985, **82**, 284.
13. W. R. Wadt and P. J. Hay, *J. Chem. Phys.,* 1985, **82**, 299.
14. J. Tomasi, B. Mennucci, and R. Cammi, *Chem. Rev.,* 2005, **105,** 2999-3094.
15. R. Dennington, T. Keith and J. Millam, 2009.